

A PRELIMINARY STUDY ON BP/CP UNCERTAINTY ANALYSIS OF WOLSONG CANDU 6 REACTORS BASED UPON RFSP-IST FINE MESH CORE MODEL

Hyung-Jin Kim¹, Dai-Hai Chung^{1*}, Jong-Hyun Kim¹ and Sung-Min Kim²

¹Atomic Creative Technology Co., Ltd., Daejeon, Korea

²Korea Hydro and Nuclear Power Co., Ltd., Daejeon, Korea

*Corresponding author: *dhchung@actbest.com*

Abstract

A preliminary study has been conducted to help estimate BP/CP uncertainty of Wolsong CANDU 6 reactors by using the WIMS/DRAGON/RFSP-IST code system. The study is focused on the effects of RFSP-IST core modeling practices, especially, in context of laying out mesh spacings associated with the structural materials in the core. The conceptual approach to figure out the effects of mesh spacing layouts associated with the structural materials is supported by the newly updated code system representing the state-of-the-art CANDU reactor physics theory and methodologies, especially, the DRAGON-IST generated incremental cross sections. The application of RFSP-IST fine mesh core model has been exercised to Wolsong Unit 2 core tracking simulations for about one year period of reactor operations. The results so obtained clearly indicate that the improved validation practices and methodology presented here could be qualified to be incorporated into the entire package of BP/CP uncertainty analysis methodologies in order to enhance the quality and reliability of error estimates related to the various topics, e.g., such as, off-line flux mapping errors.

1. Introduction

The Wolsong-1 CANDU 6 reactor (W-1) is planned to be operated based upon the Improved Technical Specifications (ITS) derived from the Improved Standard Technical Specifications (ISTS) (Ref. 1) after the major refurbishment including replacement of the pressure tube, which is currently being undertaken after nearly 25 years of service. The restart of W-1 is scheduled in spring, 2011.

The design of ISTS was initiated in response to the domestic regulatory imposition on W-1,2,3,4 issued by Korea Institute of Nuclear Safety (KINS) to establish the consistency of reactor operating practices for CANDU type heavy water reactor system with respect to the entire domestic NPP operations as one entity, so that it would be in line with the PWR, which outnumbers the CANDU PHWR, operating specifications to some extents.

The draft version of ISTS is currently under the review by KINS for approval, and during the review process it has been requested by KINS to KHNP for the establishment of new BP/CP allowance limits applicable to all the 380 channels individually in contrast to the presently applied single channel allowance limit formalism that originates from AECL. In response to KINS's request, KHNP is launching a project to conduct BP/CP uncertainty analysis based upon the 380 channel formalism. The project also includes TFD scan flux measurements to support the analytical efforts.

For the domestic reactor physics analysis the Canadian IST code system, namely, WIMS/DRAGON/RFSP-IST (Refs. 2,3,4), has been in use since about three years ago. The newly updated code system has been extensively used in replacement of the previous PPV/MULTICELL/RFSP code suite (Refs. 5,6) for the safety analysis and Phase-B pre-simulations

of W-1 to support the licensing submissions and low power commissioning tests required to restart the reactor.

For the studies intended in the present paper, the WIMS/DRAGON/RFSP-IST code suite is used and the legitimacy of using it comes from the validation results of the code suite against the previous Phase-B test measurements of W-1,2,3,4 as reported in Reference 7. The WIMS/DRAGON/RFSP-IST code system would also be in use on routine basis for W-2,3,4 in a foreseeable future.

As preparation to cope with the forthcoming tasks of BP/CP uncertainty analysis, a study has been conducted elsewhere (Ref. 8) to grasp a more realistic glance on the effects of mesh spacing layouts associated with the structural materials in the core. In [8], several models are introduced which differentiate themselves from each other by the optional featuring of mesh spacing layouts associated with the structural materials. In the present study, the most precise model, namely, the reference model with 60x98x40 mesh volumes in x-, y- and z-directions, respectively, Model R, is quoted for the application to W-2 core-tracking simulations. Model R could be alternatively considered as a RFSP-IST fine mesh core model. The WIMS/SCM (Simple Cell Methodology) fuel tables (Ref. 9) and DRAGON incremental cross sections (Refs. 3,10) are also used to complete the model setup.

In the following, the conceptual sketch in general to cope with BP/CP uncertainty analysis is laid out with respect to the reactor physics point of view, and then the fine mesh core model used for the study is briefly introduced and the simulation results are presented with discussions followed by some conclusions.

2. BP/CP Uncertainty of Wolsong CANDU 6 Reactors – Core Physics Modelling

The bundle and channel powers are constituents of transport phenomena covering fission energy release and thermalhydraulics behaviour of coolant in the reactor core. Thus, any study related to BP/CP uncertainty should be addressed to both areas together in coupled modelling practices. The very slowly changing thermalhydraulics behaviour of reactor coolant in time is normally attributed to the aging effects of mechanical components of the heat transport system that are represented by, e.g., the increase in reactor inlet header temperatures and the change in flow pattern, such as, flow rates. However, the coupling of neutronics and thermalhydraulics is not considered here, but merely the core physics part is discussed.

It is a general consensus that BP/CP uncertainty is understood as the uncertainties contained in the predicted values of bundle and channel powers produced by using the computational tools which are inherently bound with various source of errors due to the approximations and theoretical methods incorporated into the modelling of certain physical phenomena. For the reactor physics part, the WIMS/DRAGON/RFSP-IST code system is the mostly and commonly used computational tools in the CANDU reactor physics community to yield predicted values. These reactor physics computational tools are mainly built on the mathematical and theoretical modelling practices except the lattice physics area where some of nuclear data quoted for the certain nuclides could have been derived from the experimental data.

Thus, except the total reactor power measurement that is in the end used to normalize bundle power distributions in the core, the BP/CP uncertainties could be classified in terms of reactor physics modelling components. For the lattice physics code, WIMS-IST, the errors contained in the

prediction of burnup progression, which in turn represent themselves in a form of the diffusion theory compatible two-energy group macroscopic cross sections and the so-called H-Factor, contribute directly to uncertainties. For DRAGON-IST, which generates the incremental cross sections to represent reactivity devices including the structural materials present in the reactor core, the errors that contribute to uncertainties are the systematic ones that are related to the specific reactor unit characterized by its hardware components and environments in the core.

The final source of errors for reactor physics calculations as it is conceptually laid out here is rooted in the flux calculations performed by RFSP-IST. The error characteristics bound with fluxes could be split up into two components, namely, time and space dependent errors, and the results of flux calculations would be directly dependent on the RFSP-IST core model besides the lattice physics generated parameters and incremental cross sections as indicated above. The solution of two-energy-group neutron diffusion equations as built in RFSP-IST is numerically obtained and the accuracy of the solutions is governed by the number of mesh spacings and the distribution of mesh intervals in x-, y- and z-directions of the finite difference numerical scheme. With respect to this view point, an attempt has been made in [8] to derive RFSP-IST core models that account for the effects of mesh spacing layouts associated with the structural materials to the full extent.

Despite of the methodological delineations depicted here, all the predicted results obtained by using the computational tools that are built with any favourable emphases on some particular modelling practices are subject to validations against measurements in order to be qualified for the usefulness of the tools.

In Reference 11, an example of successful case in context of validations is reported where the improvement of lattice physics calculations by upgrading the lattice physics code from POWDERPUFS-V to WIMS has actually vindicated that BP/CP uncertainty could be more realistically and reliably analysed with the application of relevantly enhanced modelling practices.

3. BP/CP Uncertainty of Wolsong CANDU 6 Reactors – Off-Line Flux Mapping Errors

In RFSP-IST, the bundle power is calculated according to the following formula;

$$BP \text{ (kW)} = H_1 \times \Phi_1 + H_2 \times \Phi_2, \quad (1),$$

where $H_{1,2}$, in units of (10E-11 kW cm² s), are the WIMS-IST calculation based so-called H-Factors and $\Phi_{1,2}$, in units of (n/[cm² s]), are the volume average cell fluxes (cell average fluxes) obtained by the off-line flux mapping simulations, for fast and thermal groups, respectively. The cell volume is 28.575x28.575x49.53 cm³ that is consistent with WIMS-IST inputs for 37-element CANDU 6 fuel lattice model. The channel power is simply obtained by summing up the powers of 12 bundles loaded in a channel.

In obtaining bundle powers, the cell average fluxes used to be multiplied with H-Factors in Eq.-1 are obtained in two steps, firstly, the RFSP-IST simulation is performed which calculates the mesh cell fluxes based upon the instantaneous fuel burnup distributions in the core and the reactor configurations as defined in input, and, secondly, the instantaneous flux distributions so obtained are processed for the generation of matrices corresponding to the fundamental flux mode using *RIPPLE module of RFSP-IST. The fundamental flux mode matrices are then used with the other pre-determined higher order flux mode matrices to yield the (quasi-measured) cell average fluxes expressed in Eq.-1 by applying 102 measured vanadium detector (VD) flux readings. Besides the

contribution of measurement errors associated with VDs, the importance of the fundamental mode matrices is pronounced by the statistical fact revealed from the CANDU 6 reactor operating histories that nearly ~99% of flux mode amplitudes corresponding to the mode matrices used in the off-line flux mapping simulations are concentrated on the fundamental flux mode amplitude. Thus, the understanding of errors contained in the RFSP-IST determined instantaneous flux distributions to be used for the generation of instantaneous fundamental mode (*RIPPLE module of RFSP-IST) becomes a compelling necessity to help grasp a more realistic glance on BP/CP uncertainty.

The importance of accuracy of the flux distributions is claimed for the entire core region due to the regulatory requirement of producing BP/CP uncertainties for all the 380 channels individually, i.e., it is not confined to, e.g., the high power region. This is, from the methodological view point, in line with the estimate of flux mapping errors because 102 VDs are spatially distributed to cover the entire core region. This situation then leads to a thought that the study of the spatial effects of fluxes induced by, e.g., the top-to bottom flux tilt due to the strongly neutron absorbing structural materials in the bottom region of core would be a mandatory task for BP/CP uncertainty analysis. With respect to this view point, a study (Ref. 8) has been conducted, as mentioned earlier, to address the effects of mesh spacing layouts associated with the structural materials by creating several RFSP-IST core models based upon the optional featuring of the mesh spacing layouts. The fine mesh core model, Model R from [8], being used here counts one mesh line at each boundary of all the reactivity devices as well as the structural materials except the lightly neutron absorbing materials, such as, guide tubes.

The purpose of the present paper is addressed to the application of the fine mesh core model to core-tracking simulations in order to derive consequences of off-line flux mapping errors on the bundle power calculations.

4. Implication of Structural Material Thermal Absorptions

The RFSP-IST fine mesh core model (Ref. 8) used here is derived based upon the consideration of thermal absorptions of the structural materials, such as, e.g., nuts, brackets, locators and tensioning springs, that are in place as mechanical parts of the reactivity devices, flux detector assemblies, liquid poison injectors and moderator injection nozzles. Most of the structural materials are positioned in the bottom area of core.

Table 1 Thermal Absorption Incremental Reaction Rates of Structural Materials and Adjuster Rods ($\Delta \Sigma_{a,2}, [cm^{-1}]$, Reaction Rate = $\Phi \Delta \Sigma_{a,2} V$ [n/s] with $\Phi = 1$)

	ADJ	MCA	SOR	ZCR	MOD-INJ	LPI-BL	VFD-BL	HFD-BL	ADJ-RODS
Reaction Rates	3.1807E+03	7.3652E+02	5.1556E+03	8.7135E+02	6.3484E+02	3.5635E+02	1.5442E+03	5.3453E+02	5.6502E+03

The thermal absorption incremental reaction rates of these structural materials are summarized in Table 1 as calculated by applying flat thermal fluxes of unity.

It comes to light that the thermal absorption incremental reaction rate of the SOR structural materials alone is nearly equivalent to that of all the 21 adjuster rods, about ~91%. Note that the total sum of the thermal absorption incremental reaction rates of all the structural materials as listed in Table 1 is about ~130% more than that of all the 21 adjuster rods. Even though the actual flux levels being applied to these structural materials would be in reality lower than the flux levels at the

adjuster rod locations in the core, the observations taken here imply the importance of structural material thermal absorptions that would cause flux tilts in the core, especially, top-to-bottom tilt.

5. WIMS/SCM Fuel Tables and DRAGON Incremental Cross Sections

The WIMS-IST input parameter values that would normally correspond to CANDU 6 reactor operating conditions and be used for design and safety analysis are listed in Table 2. The SCM fuel tables as well as the DRAGON incremental cross sections to be used for simulations are generated using WIMS Utilities programs (Ref. 9) and the DRAGON-IST code (Refs. 3,10), respectively, based upon the operating conditions as listed in Table 2.

Table 2 WIMS-IST Input Parameters for SCM Fuel Table Generations

Parameter	Condition
Reactor Power [FP]	100%
W/g of Initial HE	33.4902
Coolant Temperature []	288
Moderator Temperature []	69
Fuel Temperature []	687
Coolant Density [g/cm ³]	0.80786
Moderator Density [g/cm ³]	1.08509
NU Fuel Density [g/cm ³]	10.4919
Avg. Uranium Weight [kgU/BND]	19.13525
Coolant Purity [atom%]	99.000
Moderator Purity [atom%]	99.833

6. Core-Tracking Simulations of Wolsong Unit 2

The core tracking simulations are carried out against W-2 operating history of about slightly longer than one year period, equivalent to 376 FPD, for the equilibrium core state. The flux modes used to synthesize fluxes and subsequently generate power map based upon 102 VD flux readings are the currently in W-2 production RFSP Direct Access File stored PPV time-average simulation based one and half group matrices.

However, the full two group mode matrices for the fundamental flux mode are generated through *RIPPLE module of RFSP-IST and used for off-line flux mapping simulations. This procedure could be expected to not accumulate unacceptable errors in prediction of power distribution compared to the case of using full two group flux mode matrices for the higher harmonics.

In order to model the local parameter feature within *SIMULATE module with SCMHI option, the multiple average channel models of aged core conditions of Wolsong CANDU 6 reactors are used (Ref. 12). In the CATHENA (Ref. 13) model, each core pass is made up of 7 groups, i.e., 95 channels per core pass and each pass is represented by 7 average channel groups for CATHENA inputs. The coolant densities, coolant temperatures and fuel temperatures for each bundle in 28 channel groups generated by CATHENA are then used as the local parameter inputs to the RFSP-IST core model.

Besides this spatially distributed local parameter presentation, a simple local parameter description uniformly distributed for all the bundles in the core is also used by quoting the operating conditions as given in Table 2 for comparison purposes.

The results of core-tracking simulations are summarized in Table 3. Note that the results of the uniform and distributed local parameter cases show practically the same for this particular cases.

Table 3 W-2 RFSP-IST *SIMULATE-SCMHI Option Core-Tracking Simulation Results
(Max. BP/CP and CPPF - Total Number of Flux States = 110)

Peak Max CP (MW)		Peak Max BP (kW)		Peak Max CPPF	
Uniform Local Parameter	Distributed Local Parameter	Uniform Local Parameter	Distributed Local Parameter	Uniform Local Parameter	Distributed Local Parameter
6.991(O13)	6.991(O13)	851.3(H06/6)	851.4(H06/6)	1.117(G05)	1.117(G05)
Avg Max CP (MW)		Avg Max BP (kW)		Avg Max CPPF	
6.832	6.832	824.9	825.0	1.077	1.077

7. Simulation Results – Vanadium Detector (VD) Fluxes

In Figure 1, the standard deviations (%) of RFSP-IST off-line mapped fluxes of 102 VDs calculated against the actual flux readings at the site are displayed for the core-tracking simulation intervals of total 110 cases. The average value of the standard deviations is about ~1.77% and the minimum and maximum values are 1.53% and 2.10%, which occur at Case No = 27 and 60, respectively.

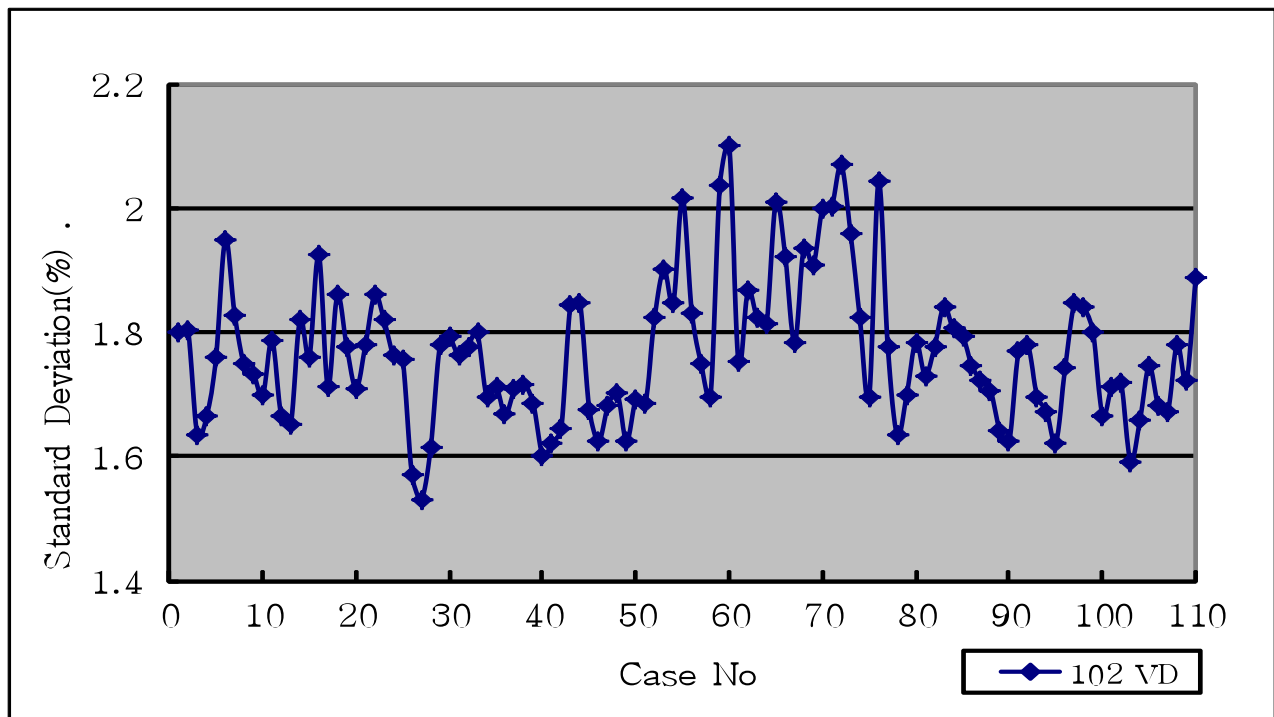


Figure 1. Standard Deviations(%) of Off-Line Mapped VD Fluxes

Table 4 Maximum Positive and Negative Differences (%) of Mapped and INTREP VD Fluxes*

Mapped VD Fluxes				INTREP VD Fluxes			
Pos		Neg		Neg		Pos	

	8.13	LH	-6.63	LH		-10.53	LH	10.21	UH
	7.45	LH	-6.37	LH		-10.29	LH	9.62	LH
	7.21	LH	-6.16	LH		-9.78	LH	9.53	UH
	6.95	LH	-5.91	LH		-9.76	LH	9.41	UH
	6.66	LH	-5.74	LH		-9.75	LH	9.37	UH
Avg	7.28		-6.16		Avg	-10.02		9.63	

* LH/UH : Lower and Upper Half of Core

The maximum positive and negative differences are given in Table 5 for the five largest values along with VD position indicators whether or not it is located in the upper half (UH) or the lower half (LH) in x-y plane of the core. The differences are calculated by using the measured VD fluxes as the reference values. The INTREP VD fluxes are interpolated by using *INTREP module of RFSP-IST at the detector sites from the cell average fluxes that are obtained through the off-line flux mapping processes.

Note that the positive and negative differences of the off-line mapped VD fluxes as shown in Table 4 reveal clear consistency that all the differences appear in the lower half of core which support the randomness of error distributions in view of the statistical observations whereas for the INTREP VD fluxes clear preference of the positive and negative difference distributions can be observed which strongly vindicates the top-to-bottom tilt of the cell average flux distributions. It is to mention that the location of VD for the second largest positive difference for the INTREP flux cases appears as LH in contrast to the other cases which outnumber this exceptional case, so that it would not convey any significance in making the conclusive observations.

As expected, the clear top-to-bottom tilt of cell average fluxes with lower flux level in the lower half of core compared to the upper half of core is confirmed here. This phenomenon must be taken into account for the final analysis of BP/CP uncertainty because the cell average fluxes are directly entered into the determination of bundle powers, see Eq.-1, even the fluxes are not validated against measurements in contrast to the case of VD fluxes. The bias structure caused by the top-to-bottom flux tilt that is to be attributed to the presence of structural materials in the bottom region of core could possibly be achieved from the systematic comparisons between the results produced by using different RFSP-IST core models, e.g., coarse and fine mesh models (Ref. 8).

Base upon the observations taken here, it is importantly suggested that for CANDU 6 reactors the measured 102 VD fluxes secure themselves as the last resource of evaluating the uncertainties inherently rooted in predicted flux values that appear as final products of various core physics characteristics related to the constituents of model used to calculate fluxes.

The differences between the mapped and INTREP VD average fluxes as listed in Table 5 are 2.74% and -3.45% for the positive and negative differences, respectively.

8. Simulation Results - Flux Tilts

The results obtained from W-2 core-tracking simulations by using the RFSP-IST fine mesh core model are further analysed in-depth in context of zonal and VD flux distributions. In this analysis, the off-line flux mapping calculations are directly compared against the actual flux measurements based upon 102 VD flux readings in context of flux tilts that could be understood as a fair measure

to make judgements on the quality and reliability of model used with emphasis on the effects of mesh spacing layouts associated with the structural materials (Ref. 8).

During reactor operations, various decisions, such as, e.g., fuel managements and shim operations, are made based upon the flux and power distribution in 14 zones. The importance of mapped VD fluxes is earlier discussed. Thus, the analyses are carried out here with examples of zonal and VD fluxes in terms of flux tilts.

The flux tilt at location i relative to another location j in core is defined as follows;

$$FT_{ij} (\%) = (F_j - F_i) / (F_j + F_i) * 100, \quad i=1 \text{ to } N \text{ and } j=i+1 \text{ to } N,$$

where N corresponds to the total number of VD locations of interest, normally, $N=102$. The zonal flux ZF_k is the sum of VD fluxes F_i in zone k . For zones, the index k is $k=1$ to 14 . If there are, e.g., M detectors in zone k , then the index i is $i=1$ to M to sum up VD fluxes for ZF_k .

In order to conduct systematic observations, the definition of difference between the mapped and INTREP zonal and VD flux tilt at the location i associated with the location j is introduced by using the measured flux tilt value ZFT_{ij} and FT_{ij} as the reference one;

$$\text{Mapped Tilt Diff}_{ij} (\%) = \text{Mapped Tilt}_{ij} (\%) - \text{Measured Tilt}_{ij} (\%), \text{ and}$$

$$\text{INTREP Tilt Diff}_{ij} (\%) = \text{INTREP Tilt}_{ij} (\%) - \text{Measured Tilt}_{ij} (\%),.$$

The average tilt differences and the corresponding standard deviations are given in Table 5 for five cases. For convenience here the VD IDs are numbered from 1 to 56 for UH and 57 to 112 for LH, respectively, although the ID numbering is differently structured in Official Design Manuals of CANDU 6 reactor. Note that 10 VDs whose vertical centres are located right on the x-z plane at the midpoint in y-direction are counted twice for UH and LH, respectively.

The four VD cases differentiate themselves as follows;

- All to All : $i = 1 \text{ to } 101$ and $j = i+1 \text{ to } 102$, (5151 FT_{ij}),
- UH to UH : $i = 1 \text{ to } 55$ and $j = i+1 \text{ to } 56$, (1540 FT_{ij}),
- UH to LH : $i = 1 \text{ to } 56$ and $j = 57 \text{ to } 112$, (3136 FT_{ij}) and
- LH to LH : $i = 57 \text{ to } 111$ and $j = i+1 \text{ to } 112$, (1540 FT_{ij}).

Table 5 Average and Standard Deviation of Zonal and VD Flux Tilt Differences (%)

Case	Mapped		INTREP		INTREP-Mapped
	Avg	St. Dev	Avg	St. Dev	St. Dev Diff
ZONE	0.085	0.310	0.174	1.354	1.044
VD - UH to UH	-0.005	1.171	0.358	2.041	0.870
VD - All to All	-0.026	1.226	0.088	1.991	0.764
VD - UH to LH	0.006	1.252	-1.044	1.831	0.579
VD - LH to LH	-0.004	1.346	-0.111	1.575	0.229

The average differences of mapped flux tilts show the largest value for the zonal flux tilt case and the values for VD flux tilt cases are all nearly zero. The average differences of INTREP flux tilt cases are noticeably larger than the values of mapped flux tilt cases with the largest value of -1.044 for the VD – UH to LH case, which again vindicates the effect of top-to-bottom flux tilt of the cell average flux distributions.

The standard deviation of zonal flux tilts show smaller values compared to the VD flux tilt cases both for the mapped and INTREP flux tilt cases due to the fact that the zonal fluxes are summed up out of VDs that are located nearby each other in the corresponding zones. Out of 14 zones, zones 4 and 11 have the most number of VDs, 12. However, this number is outnumbered by 56 VDs either in UH or LH of the core.

For the mapped VD flux tilts, the smallest standard deviation occurs for the case of VD – UH to UH and vice versa for the INTREP flux tilt cases. This observation is valid also for the largest and smallest standard deviation for the mapped and INTREP VD flux tilt cases, i.e., VD – LH to LH cases, respectively. The differences of the standard deviations between the cases VD – UH to UH and VD – LH to LH are $1.171 - 1.346 = -0.175\%$ and $2.041 - 1.575 = +0.466\%$ for the mapped and INTREP flux tilts, respectively. This supports a better consistency of the mapped VD flux distributions, which in turn exposes the inferior quality of INTREP VD flux distributions against the former ones.

In Table 5 the differences between the standard deviations of mapped and INTREP VD flux tilts are given in the last column. The largest and smallest differences occur again for VD – UH to UH and VD – LH to LH cases, respectively, which again clearly reflect the effect of top-to-bottom flux tilt of the cell average flux distributions. The largest difference of 0.870% could be absorbed as one of the uncertainty components that would have been rooted in the RFSP-IST calculated bundle powers.

In Figure 2 the behaviour of differences between the mapped and INTREP VD flux tilt standard deviations for VD – UH to UH case is graphically displayed for W-2 core-tracking simulations.

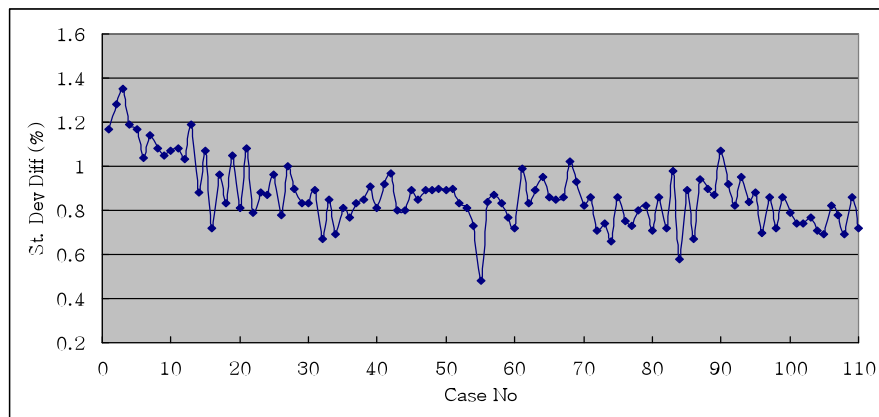


Figure 2 Differences between Mapped and INTREP VD Flux Tilt Standard Deviations
 for VD – UH to UH Case (see Table 5)

The difference starts initially with noticeably higher values compared to the average value, but then gradually decreases until around Case No = ~30 and from there on stays mostly between 0.6% and 1.0%. The reason for the initially higher values of differences could possibly be attributed to the model switching from PPV/RFSP to WIMS/RFSP-IST, and the switching might require some simulations until the initial burnup distribution in the core imported from the PPV/RFSP model into the WIMS/RFSP-IST local parameter model would have fully settled down.

One further consideration is offered here that since the INTREP fluxes at certain points in the core are interpolated by using the parabolic polynomial relationship of cell average fluxes in the space of interest at and/or around the interpolation point, the INTREP fluxes are directly bound with the

characteristics of cell average fluxes. However, the ratio of lattice cell boundary point fluxes, e.g., the fluxes at detector locations, to the lattice cell average fluxes are dependent on the fuel burnup of lattice cells. Thus, it would be interesting subject to bring the WIMS lattice cell calculation based fuel burnup dependent ratio of the lattice cell boundary fluxes to the lattice cell average fluxes into INTREP VD flux interpolations and confirm whether or not the quality of INTREP VD fluxes would consequently be improved against the mapped VD fluxes (see Table 5).

9. Conclusions

In the present paper, a preliminary study has been conducted to grasp glance on better understanding of the effects of top-to-bottom flux tilt associated with the structural materials of Wolsong CANDU 6 reactors by using RFSP-IST fine mesh core model.

The result of comparisons between the mapped and INTREP VD fluxes obtained from W-2 core-tracking simulations show that the uncertainty imposed on BP/CP calculations using RFSP-IST would be about 0.870% due to the top-to-bottom flux tilt phenomena in the core.

The methodology used here to derive one of the BP/CP uncertainty components could be applied to various regions of the core, e.g., high power, periphery, top, bottom, side regions and any other relevant regions of interest, so that it would be useful to derive the realistically more reliable estimate of BP/CP uncertainty for all the 380 channels.

10. References

- [1] "CANDU Type Pressurized Heavy Water Reactor Nuclear Power Plant Standard Technical Specification Guidelines", Prepared by Atomic Creative Technology Co., Ltd., October 2009.
- [2] D. Altiparmakov, "New Capabilities of the Lattice Code WIMS-AECL", Proc. Int. Conf. on Reactor Physics, Nuclear Power: A Sustainable Resource, PHYSOR-2008, Interlaken, Switzerland, September 14-19, 2008.
- [3] G. Marleau, A. Hebert, and R. Roy, "A User Guide for DRAGON", Report IGE-174, Rev.5, École Polytechnique de Montréal, April 2000.
- [4] B. Rouben, "RFSP-IST, The Industry Standard Tool Computer Program for CANDU Reactor Core Design and Analysis", Proceedings of the 13th Pacific Basin Nuclear Conference, Shenzhen, China, Oct. 21-25, 2002.
- [5] D.B. Miller and E.S.Y. Tin, "POWDERPUFS-V User's Manual", AECL Report TDAI-31 Part 2, 1976 March.
- [6] A.R. Dastur et al., "MULTICELL User's Manual", AECL Report TDAI-208, 1979.
- [7] D.H. Chung, B.G. Kim, S.M. Kim, H.B. Suh, H.S. Kim and H.J. Kim, "Experience with Wolsong-1 Phase-B Pre-Simulations using WIMS/DRAGON/RFSP-IST Code Suite", 31st Annual CNS Conference, Montreal, QC, Canada, May 24 - 27, 2010.
- [8] D.H. Chung, H.J. Kim and S.M. Kim, "Effects of Structural Materials on BP/CP Uncertainty Studies for RFSP-IST Modelling of Wolsong CANDU 6 Reactors", Paper to be presented, 32nd Annual CNS Conference, Niagara Falls, Ontario, Canada, June 5-8, 2011.

- [9] T. Liang, W. Shen, E. Varin and K. Ho, "Improvement and Qualification of WIMS Utilities", 29th Annual CNS Conference, Toronto, Ontario, June 1 - 4, 2008.
- [10] M. Dahmani, "Qualification and Development Plan for the T16MAC Version 1.0", AECL Report 153-113190-PLA-002, Rev. 0, 2007 November.
- [11] C. Olive, L. Wilk, P. Sermer, D.H. Chung, S. Goodchild, M.K. O'Neill and R. Laidler, "Upgrades to the Simulation Of Reactor Operation (SORO) code for core-follow simulations of Ontario Power Generation and Bruce Power Reactors", IAEA TM on ASAM, 20071030-1102, KINS, Daejeon, Korea.
- [12] S. R. Kim and B. J. Moon, "CATHENA Multiple Average Channel Model", 59RF-03500-AR-041 Rev.1, KEPCO-EC, 2009.04.30.
- [13] B. Hanna, "CATHENA: A Thermalhydraulic Code for CANDU Analysis", J. Nuclear Engineering and Design, 180, p113-131.